the tunneling step (the second step). The correlation of ln k_H with ln K suggests that it is the third step which mainly shares rate-limiting character with the second, rather than the first. In the nonhydroxylic solvents translational and rotational solvent motions, which are responsive to bulk viscosity,[33] are important components of the heavy atom reorganization steps. We suggest that the hydroxylic solvents disable the pretunneling configuration or stabilize the posttunneling configuration, by hydrogenic motions which are faster than molecular rotation and unrelated to bulk viscosity.[34] In the theoretical section we have shown that the observed pattern of isotope effects could be produced by the competition of the tunneling step with either or both of the spontaneous heavy atom reorganization steps.

Other things being equal, eq 2 anticipates that high-viscosity solvents, which give lower limit values for k_H/k_D, should also give lower values of k_H' than solvents which give upper limit values of k_H/k_D. In the lower limit cases an additional bottleneck has appeared. We recognize, of course, that the solvents might also influence k in more conventional, quasi-thermodynamic ways.[4] Some of those influences are also reflected in K. Those may be removed by using k_H' instead of k_H. In fact, all the lower limit solvents give significantly smaller values of k_H' than do solvents which give larger values of k_H/k_D although the differences are not large.

Since solvent viscosity, in general, is correlated with solvent density, the isotope effects and rates cited in Table I correlate with the latter to about the same degree as they do with the former. This raises the possibility that the kinetic quantities are responding to internal pressure, a quasi-thermodynamic solvent property,[35] rather than to viscosity, a dynamic property. At the moment we see no rigorous way to exclude this possibility. However, it seems unattractive because it seems likely that an increase in internal pressure would increase the rate of our reaction, since it almost certainly has a negative volume of activation.[36] Similarly, the present results do not require that the second stage be a tunneling process. They strongly suggest only some sort of two- or three-stage process, in which solvent characteristics determine the rate-limiting stage. Without this we see no way that two very different sets of isotope effects could be generated with such small ranges of K and k_H. The suggested model accounts for the observations and seems to be in general accord with theory and previous work on this reaction. Further tests are in progress.

(33) Bauer, D. R.; Alms, G. R.; Brauman, J. I.; Pecora, R. *J. Chem. Phys.* **1974**, *60*, 2255.
(34) (a) Maroncelli, M.; Fleming, G. R. *J. Chem. Phys.* **1988**, *89*, 5044. (b) Hynes, J. T. *J. Phys. Chem.* **1986**, *90*, 3701.
(35) Levine, I. N. *Physical Chemistry*, 3rd ed.; McGraw Hill: New York, 1988; pp 122-124.
(36) Isaacs, N. S. *Isotopes in Organic Chemistry*; Buncel, E., Ed.; Elsevier Scientific Publishing Co.: Amsterdam, 1984; Vol. VI, p 96.

Inclusion by Cyclodextrins To Control Dye Aggregation Equilibria in Aqueous Solution†

William G. Herkstroeter,* Peter A. Martic,‡ and Samir Farid*

Contribution from the Corporate Research Laboratories, Eastman Kodak Company, Rochester, New York 14650. *Received July 17, 1989*

Abstract: Oxazine 1 perchlorate (A) and oxazine 170 perchlorate (D) were selected to investigate the influence of cyclodextrins (CDs) on the dyes' aqueous solution aggregation equilibria. Through equilibrium processes, these days form inclusion complexes with β- and γ-CD. The amphiphile hexane sulfonate can be coincluded with D in γ-CD. We report determination of the stoichiometries of all inclusion complexes and measurement of all equilibrium constants; temperature effect data on some of the latter are also included. This study clearly demonstrates that proper size matching between the guest and the host's cavity leads to substantially larger equilibrium constants. All experimental measurements for each dye rely on changes in absorption intensities of the individual long wavelength monomer and dimer absorption bands. Because H-dimers are formed, the dimer absorption bands are blue-shifted relative to the monomer bands and only the monomers fluoresce. Although, in the absence of CDs, A is mostly monomer and D is mostly dimer or larger aggregate, the intercession of CDs can be used to force A to mostly dimer and D to mostly monomer.

In recent years, there has been considerable interest in cyclodextrin (CD) inclusion complexes, as they can alter the physical properties and chemical reactivities of guest molecules.[1-6] Many organic compounds can be included in the cavities of these cyclic oligosaccharides because of the hydrophobic attraction of their interiors. In aqueous solutions, equilibria are established between uncomplexed molecules and inclusion complexes; frequently, guest and host combine to form two or more complexes that differ in their stoichiometries and degree of stabilization. The stoichiometries, the magnitude of the equilibrium constants, and the degree of protection afforded the included compounds depend to a large extent on the fit of the guest molecules into the cavities of the cyclodextrins. The three common CDs, designated α, β, and γ, consist of six, seven, and eight glucose units, respectively. Instead of cylinders, truncated cones provide a better approximation to CD shapes. The internal diameter range is 4.2-8.8 Å in α-CD, 5.6-10.8 Å in β-CD, and 6.8-12.0 Å in γ-CD; the height of each CD is 7.8 Å.[7]

The ability to alter dye solubilities and to shift equilibria among dye monomer, dimer, and higher aggregate forms makes CD

† Presented at the 17th Northeast Regional Meeting of the American Chemical Society, Rochester, NY, November 8-11, 1987.
‡ Present address: Analytical Technology Division, Eastman Kodak Company, Rochester, NY 14650.

(1) Bergeron, R. J. *J. Chem. Educ.* **1977**, *54*, 264.
(2) Bender, M. L.; Komiyama, M. *Cyclodextrin Chemistry*; Springer-Verlag: New York, 1978.
(3) Szejtli, J. *Starch/Staerke* **1978**, *30*, 427.
(4) Saenger, W. *Angew. Chem., Int. Ed. Engl.* **1980**, *19*, 344.
(5) Tabushi, I. *Acc. Chem. Res.* **1982**, *15*, 66.
(6) Pagington, J. A. *Chem. Brit.* **1987**, *455*.
(7) Ramamurthy, V. *Tetrahedron* **1986**, *42*, 3753.

0002-7863/90/1512-3583$02.50/0

Scheme I

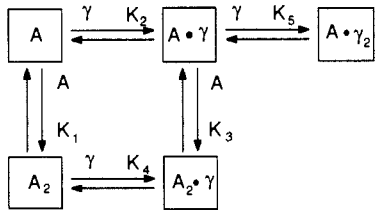

inclusion complexation particularly important when working with aqueous solutions of organic dye molecules. Consequently, such inclusion complexation can affect those dye spectroscopic characteristics and dye photophysical properties influenced by the state of dye aggregation such as electronic absorption spectra and fluorescence quantum yields.

Quantitative analyses of the equilibria of dye–CD inclusion complexation are frequently complicated by the simultaneous presence of several different complexes, and only limited data are available about the kinetics and thermodynamics of such systems. Using selected dyes, we report herein quantitative data dealing with CD effects on these dyes' monomer–dimer equilibria. This involves determination of inclusion complex stoichiometries and measurement of all equilibrium constants. Some temperature effects as well as the coinclusion of an amphiphile and dye by γ-CD are also detailed.

The two dyes under investigation are oxazine 1 perchlorate (A) and oxazine 170 perchlorate (D). They were selected because the monomer and dimer forms of each dye have distinct absorption bands with widely separated maxima. Also, and more signifi-

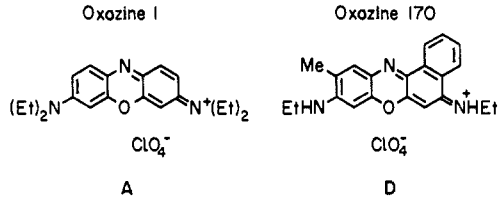

A D

cantly, these dyes, although relatively similar in structure, offer contrasting behavior: A exists mostly in monomer form in aqueous solutions of moderate concentrations, whereas D has a high propensity toward dimerization or even higher aggregation. Even at relatively low concentrations, D is present only partially in monomer form.

Results

Inclusion Complexes of Oxazine 1 Perchlorate (A). The absorption spectrum of A in aqueous solution indicates that up to a concentration of approximately 1×10^{-5} M almost all the dye molecules are in monomer form. Even with ten times as much dye in solution, less than 10% of the dye molecules are converted to dimer. Addition of γ-CD to an aqueous solution of A leads to a dramatic inversion of the dimer-to-monomer ratio. At γ-CD concentrations up to approximately 1×10^{-2} M, the data can be interpreted in terms of equilibria between three species: uncomplexed A, 1:1 complex A·γ, and 2:1 complex A_2·γ. On the other hand, as the concentration of γ-CD rises above 1×10^{-2} M, progressively higher deviations occur between experimental data and calculated values based on such a scheme. However, these deviations can be attributed to formation of the minor 1:2 complex A·γ_2. Thus, all data for A in the presence of γ-CD can be explained in terms of Scheme I.

Quantitative evaluation of the equilibria of Scheme I required measurement of individual absorption spectra of the monomer and dimer forms of A. As indicated earlier, at concentrations less than 1×10^{-5} M, virtually all of the dye is in monomer form. Furthermore, in the presence of β-CD, where the 1:1 complex A·β predominates, the spectrum is indistinguishable from that of uncomplexed A. Therefore, it is reasonable to assume that the same monomer absorption spectrum also applies to A·γ. We also make the same assumption for A·γ_2, which, even at relatively high γ-CD concentrations, is present only at low levels.

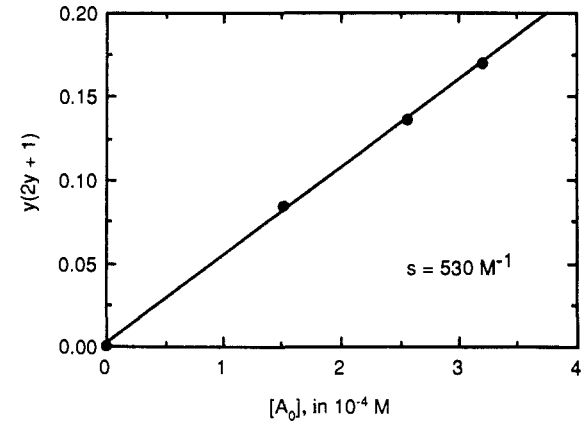

Figure 1. Plot of $y(2y + 1)$ versus $[A_0]$ in the absence of CD. The slope is equal to K_1.

Determination of the dimer spectrum is complicated because complete conversion to either A_2 or A_2·γ is not possible. The former is formed in measurable quantity only in the absence of γ-CD and then, as noted previously, only as a small fraction of the total dye concentration. When A is in the presence of γ-CD, A_2·γ becomes the only measurable form of A dimer. Maximum conversion to A_2·γ is best achieved at a high concentration of A in the presence of γ-CD. At constant dye concentration, the fraction of dimer passes through a maximum as the concentration of γ-CD is raised. Even under the most favorable conditions, where the equilibria are shifted to maximize the formation of A_2·γ, residual monomeric species still contribute measurably to the overall absorption spectrum; appropriate corrections must be applied to such a spectrum to establish the spectrum of A dimer alone.

Experimental analyses are based on the ratio R of the absorbance at the dimer absorption maximum at 599 nm (λ_1) and the monomer absorption maximum at 654 nm (λ_2). This absorbance ratio R is related to the ratio y of dimer-to-monomer concentrations as given by eq 1. In eq 1, a is the ratio of the extinction

$$y = \frac{c(R - a)}{b - R} \tag{1}$$

coefficients of the monomer at λ_1 and λ_2, b is the corresponding ratio for the dimer, and c is the ratio of the extinction coefficients of monomer-to-dimer at λ_2. The experimentally determined values of a, b, and c at 10 °C are 0.414, 5.5, and 3.0, respectively.[8]

An additional parameter z, the square of which is defined as the ratio $[A_{monomer}]^2/[A_{dimer}]$, is related to y according to eq 2, where $[A_0]$ is the total concentration of dye A.

$$z^2 = \frac{[A_0]}{y(2y + 1)} \tag{2}$$

We begin the analysis of Scheme I with K_1. The determination of K_1 is based on measurements of R at several different dye concentrations, but with no CD present. Under these conditions, K_1 is equal to $1/z^2$. Thus, by plotting $y(2y + 1)$ versus $[A_0]$ according to eq 3, the slope is equal to K_1. Figure 1 is such a

$$y(2y + 1) = K_1[A_0] \tag{3}$$

plot for measurements at 10 °C, and the slope is 530 M^{-1}. These measurements were also carried out at 6, 14, 18, and 25 °C; and the corresponding K_1 values are 594, 472, 423, and 350 M^{-1}, respectively. From the Figure 2 plot of log K_1 versus $1/T$, ΔH for this equilibrium is −4.6 kcal/mol and ΔS is −3.8 cal/(deg·mol).

In the presence of γ-CD, A_2·γ accounts for the substantial increase in the concentration of the dimer form of A. The parameter z is related to the concentration of γ-CD and the equilibrium constants of Scheme I according to eq 4. Because the concentration of γ-CD is always in substantial excess over that

(8) The value of a changes with temperature. At 6, 14, 18, and 25 °C, a is taken as 0.410_5, 0.417, 0.421, and 0.426_5, respectively.

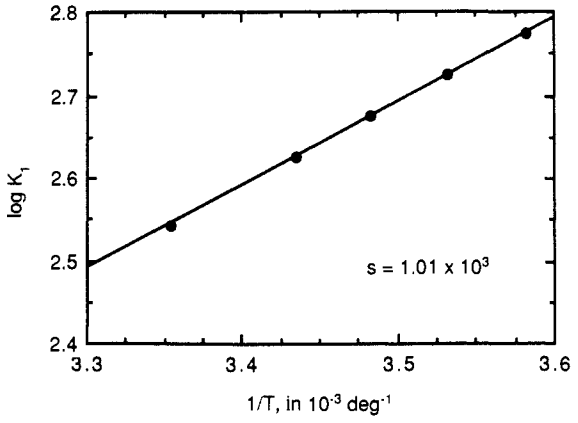

Figure 2. Plot of log K_1 versus $1/T$. ΔH is equal to the slope multiplied by $2.303R$.

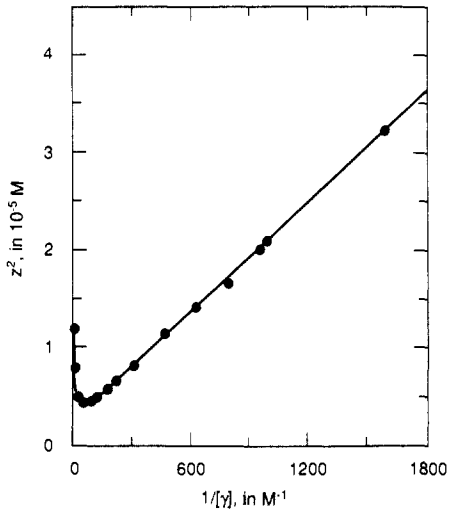

Figure 3. Plot of z^2 versus $1/[\gamma]$. The slope and intercept of the straight line for low $[\gamma]$ are used to determine K_2 and K_3 (see text).

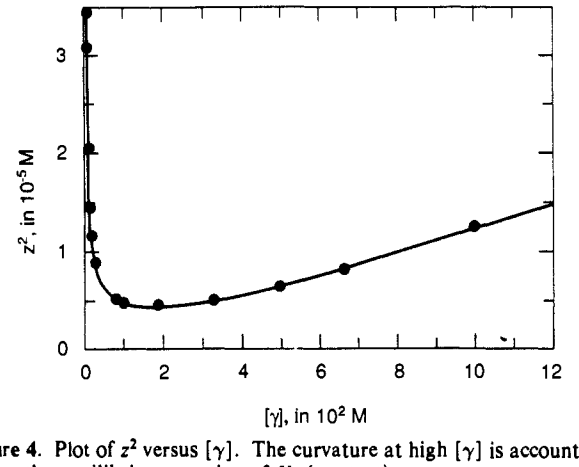

Figure 4. Plot of z^2 versus $[\gamma]$. The curvature at high $[\gamma]$ is accounted for by the equilibrium reaction of K_5 (see text).

Table I. Temperature Variation of Scheme I Equilibrium Constants[a,b]

T, °C	K_1, M^{-1}	K_3, M^{-1}	K_4, M^{-1}
6	5.9×10^2	1.24×10^6	1.17×10^5
10	5.3×10^2	9.4×10^5	9.9×10^4
14	4.7×10^2	7.1×10^5	8.4×10^4
18	4.2×10^2	5.3×10^5	7.0×10^4
25	3.5×10^2	3.1×10^5	5.0×10^4

[a] Between 6 and 25 °C, K_2 was invariant within experimental error at 56 M^{-1}. [b] K_5 was measured only at 10 °C, where its value is 2.6 M^{-1}.

$$z^2 = \frac{2}{K_3} + \frac{1}{K_2K_3}[\gamma]^{-1} + \frac{K_2 + 2K_5}{K_3}[\gamma] + \frac{2K_2K_5}{K_3}[\gamma]^2 + \frac{K_2K_5^2}{K_3}[\gamma]^3 \quad (4)$$

of A, the initial and the equilibrium concentrations of γ-CD can be taken as the same. On the basis of the magnitudes of the equilibrium constants in eq 4 and at concentrations of γ-CD less than 5×10^{-3} M, the final three terms in this equation are negligible compared with the first two. Accordingly, a plot of z^2 versus $[\gamma]^{-1}$ should be nearly linear for low $[\gamma]$. This prediction is satisfied in Figure 3, whose slope and intercept yield K_2 and K_3 values of 56 and 9.4×10^5 M^{-1}, respectively, for data measured at 10 °C.

The remaining unknown in eq 3, the minor equilibrium constant K_5, was determined by comparing experimental z^2 values with calculated curves assuming different values for K_5 in eq 3. The best fit of the data at 10 °C was obtained for K_5 equal to 2.6 M^{-1}. The curves in Figures 3 and 4 were calculated on the basis of K_2, K_3, and K_5 of 56, 9.4×10^5, and 2.6 M^{-1}, respectively. Agreement between the experimentally measured points and the calculated curves is evident.

According to Scheme I, K_2K_3 is equal to K_1K_4. Since the first three have been determined, it follows that K_4 has the value 9.9×10^4 M^{-1} at 10 °C.

From these equilibrium constants, the maximum fraction of the dye in dimeric form at this temperature is reached when $[\gamma]$ is 0.0162 M. At this concentration of γ-CD, the parameter z reaches a minimum value of 4.44×10^{-6} M^{-1}. Accordingly, the fraction of molecules in dimeric form for $[A_0]$'s of 10^{-5} and 10^{-4} are 62 and 86%, respectively.

The formation of the dimeric inclusion complex is strongly temperature-dependent as indicated by the changes in the absorption spectra shown in Figure 5. To determine the temperature variation of K_2 and K_3, additional plots of z^2 versus $[\gamma]^{-1}$ were constructed from data measured at 6, 14, 18, and 25 °C. The corresponding values of K_3 are listed in Table I and change by a factor of 4, whereas K_2 is invariant within experimental error. The temperature dependence of K_4 is established by dividing the product K_2K_3 at different temperatures by the corresponding value of K_1; results are listed in Table I. The temperature dependence of the relatively weak equilibrium constant K_5 was not measured.

For K_2, ΔH must be close to zero, whereas ΔS is positive at approximately 8 cal/(deg·mol). The slope of the linear plot of log K_3 versus $1/T$ (Figure 6) corresponds to ΔH for this dimer-forming equilibrium of −12 kcal/mol and ΔS of −16 cal/(deg·mol). From a like plot for K_4, ΔH for this equilibrium reaction is −7.5 kcal/mol and ΔS is −3.6 cal/(deg·mol). These thermodynamic parameters are summarized in Table II.

We also determined for A the influence of self-association upon the fluorescence quantum yield. Our experiment used a series of solutions containing the same initial concentration of A and varying concentrations of γ-CD so that the monomer-to-dimer ratio of A varied; excitation at an isosbestic point showed that the fluorescence intensities were directly proportional to the fraction of monomer in each solution. This result indicates that the dimer does not fluoresce.

Oxazine 170 Perchlorate. The contrasting behavior of D is such that D, in the absence of CDs, favors dimers in the aqueous equilibrium of eq 5. The nature of these dimers is to adhere to

$$2D \rightleftharpoons D_2 \quad (5)$$

the surface of glass containers so as to make measurements of absorption spectra unreliable. To explain this poor solubility of D in aggregate form, it is entirely possible that eq 5 is incomplete and that aggregation beyond the dimer stage occurs with D.

To gain control of the aqueous equilibrium reactions of D, γ-CD can be used to solubilize D in dimer form. An example of an absorption spectrum run under such conditions is curve 1 of Figure 7. That this spectrum is caused by D in dimer form is certain, because aggregates larger than dimers simply do not fit into the γ-CD cavity.

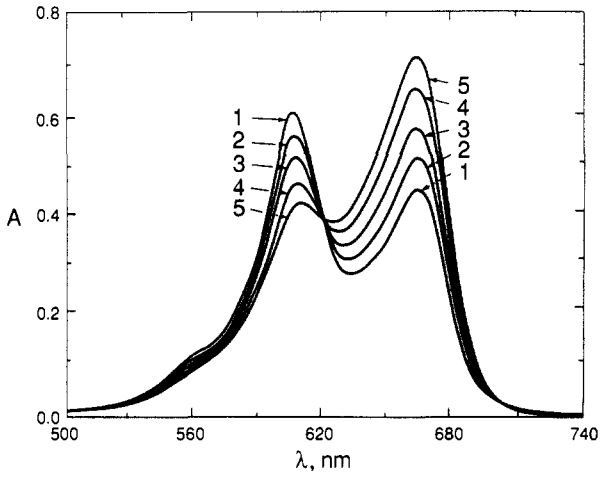

Figure 5. Temperature-dependent absorption spectra of 8.0×10^{-6} M A in the presence of 8.0×10^{-3} M γ-CD. Curves 1–5 correspond to measurements at 10, 18, 25, 35, and 45 °C, respectively.

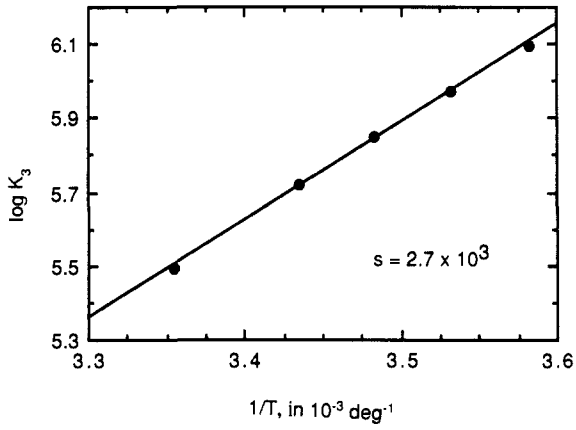

Figure 6. Plot of log K_3 versus $1/T$. ΔH is equal to the slope multiplied by $2.303R$.

Table II. ΔH and ΔS for Scheme I Equilibrium Reactions[a]

equilibrium reaction	ΔH, kcal/mol	ΔS, cal/(deg·mol)
K_1	−4.6	−3.8
K_2	~0	+8
K_3	−12	−16
K_4	−7.5	−3.6

[a] ΔH and ΔS were not measured for the reaction associated with K_5.

We now present two methods that involve CDs to shift the overall equilibrium of D to favor monomer forms. Such shifts can be effected by adding either β-CD or hexane sulfonate (X) to D solutions that already contain γ-CD.

The remaining absorption curves of Figure 7 show the effectiveness of progressively higher concentrations of β-CD in shifting equilibria for D toward monomer forms. To explain these and other results for D in the presence of both β-CD and γ-CD or either one alone, we rely on the equilibrium scheme shown in Scheme II. This scheme includes only those species required by our data.

For our experimental measurements, we again rely on changes in the intensities at the band maxima of the dimer and monomer absorption bands (583 and 623 nm, respectively). At any fixed total concentration of dye, conversion to dimer passes through a maximum with increasing concentrations of γ-CD, whereas the concentration of monomer can be maximized by β-CD. Even when the conversion to either dye form is maximized, small amounts of the other dye form are still present, and corrections must still be applied to determine the individual dimer and monomer spectra. We assume that CD inclusion does not change the extinction coefficients of the dimer and monomer forms of D at their respective absorption maxima.

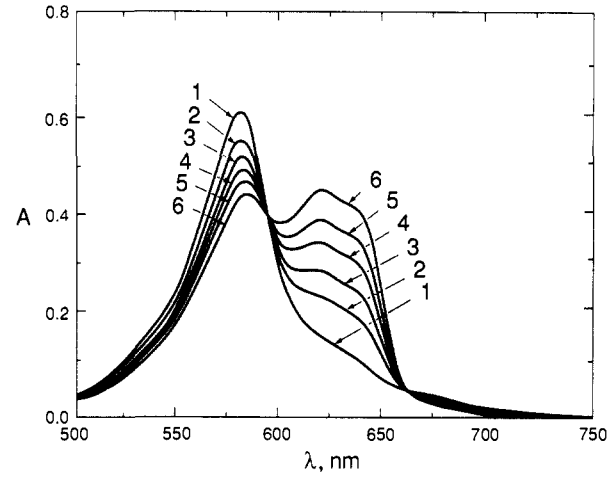

Figure 7. Absorption spectra of 1.14×10^{-5} M D in the presence of 1.3×10^{-4} M γ-CD in curve 1 and with the addition of 0.0023, 0.0040, 0.0063, 0.0085, and 0.013 M [β] in curves 2, 3, 4, 5, and 6, respectively.

Scheme II

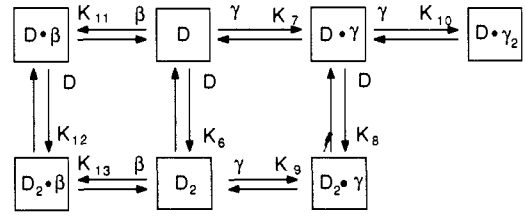

To convert the experimental ratios R to their corresponding y ratios, eq 1 is used with a, b, and c equal to 0.59, 5.1, and 2.5, respectively, at 25 °C. The experimental determination of the parameter z is based on eq 2 with $[D_0]$ substituted for $[A_0]$; z is related to the concentrations of β-CD and γ-CD and the equilibrium constants of Scheme II according to eq 6. Since K_6K_9

$$z = \frac{1 + K_7[\gamma] + K_7K_{10}[\gamma]^2 + K_{11}[\beta]}{\sqrt{K_6 + K_6K_9[\gamma] + K_6K_{13}[\beta]}} \quad (6)$$

$= K_7K_8$ and $K_6K_{13} = K_{11}K_{12}$, this expression includes all equilibrium constants. Through various simplifications and approximations, we now show that all eight equilibrium constants are amenable to experimental determination.

A logical place to begin is the determination of K_6 in the absence of CDs. Under such conditions, eq 1 with $[D_0]$ in place of $[A_0]$ is expected to apply so that experimentally determined y values at different D concentrations are all that should be required to determine K_6. Our attempt to follow this procedure, despite using dye concentrations well below 1×10^{-6} M, was still plagued by partial adherence of D aggregates to the walls of absorption cells and consequent, imprecise absorption measurements. On the basis of such measurements, K_6 cannot be more precisely defined than to say it is bounded between 1×10^4 and 1×10^5 M^{-1}. Another procedure described below provides for an alternate determination of K_6.

Consider next the situation with $[D_0]$ fixed and relatively low, variable and low concentrations of γ-CD, and no β-CD. To determine the product K_7K_8, we use the following abbreviated analogue of eq 4

$$z^2 \approx \frac{2}{K_8} + \frac{1}{K_7K_8}[\gamma]^{-1} \quad (7)$$

where K_7, K_8, and K_{10} are substituted for K_2, K_3, and K_5, respectively, and the final three terms are regarded as negligible and are dropped. Again by analogy, this time to Figure 3, the reciprocal of the slope of a plot of z^2 versus $[\gamma]^{-1}$ has the value 5.7×10^{10} M^{-2} and is equal to the products K_7K_8 and K_6K_9. The intercept is too small with respect to experimental values of z^2

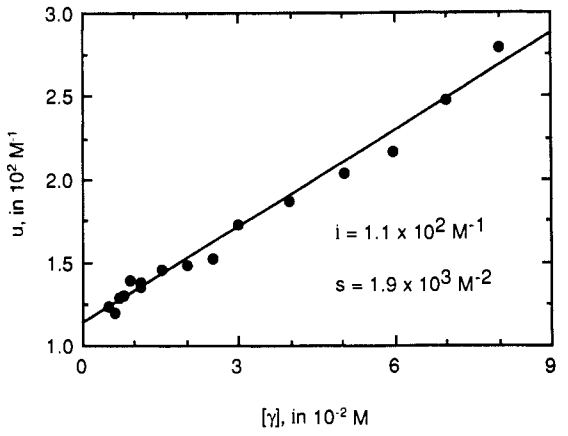

Figure 8. Plot of u versus $[\gamma]$. The intercept is equal to K_7 and the slope is equal to the product K_7K_{10}.

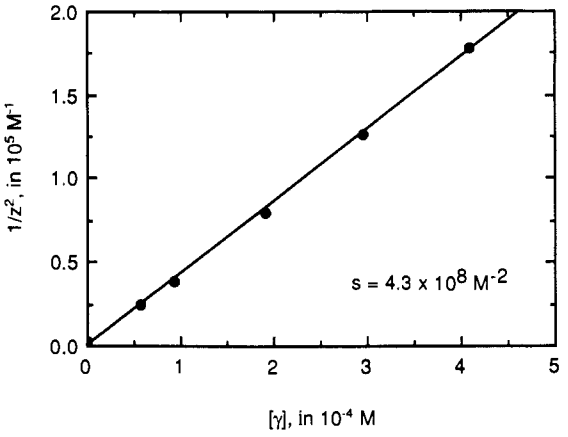

Figure 9. Plot of $1/z^2$ versus $[\gamma]$. See eq 9 for the relationship between the slope and K_{11}.

plotted along the ordinate to be used as a reliable basis for determining K_8 alone.

Next, we consider the effects of higher concentrations of γ-CD. Under these conditions, K_{10} becomes measurable. The terms of eq 6 can be reordered to yield eq 8, where u, whose terms are all

$$u = \frac{z(\sqrt{K_6K_9[\gamma]}) - 1}{[\gamma]} \approx K_7 + K_7K_{10}[\gamma] \qquad (8)$$

either measurable or known, is defined as written. The approximation is that K_6 is negligible with respect to the product $K_6K_9[\gamma]$. The intercept from the plot of u versus $[\gamma]$ (Figure 8) is 1.1×10^2 M^{-1}, and this value is assigned to K_7; the slope of 1.9×10^3 M^{-2} is assigned to the product K_7K_{10} so that K_{10} must be 17 M^{-1}. Because K_7 is now known, K_8 must be equal to 5.1×10^8 M^{-1}.

We continue our experiments keeping $[D_0]$ fixed and relatively low, but we now add a fixed and relatively high concentration of β-CD; the concentration of γ-CD is again kept low, but it is a variable. After making the approximations in eq 6 that $K_7[\gamma]$ and $K_7K_{10}[\gamma]^2$ are small with respect to $K_{11}[\beta]$ and that K_6 is small with respect to $K_6K_9[\gamma]$ and $K_6K_{13}[\beta]$, we derive eq 9. The slope of the plot of $1/z^2$ versus $[\gamma]$ (Figure 9) is 4.3×10^8, and this yields a value of 1.05×10^3 M^{-1} for K_{11}.

$$\frac{1}{z^2} \approx \frac{K_6K_{13}[\beta] + K_6K_9[\gamma]}{(1 + K_{11}[\beta])^2} \qquad (9)$$

When $[\beta]$ is a variable in the absence of γ-CD, the following equation results from algebraic reordering of terms in eq 6; v is defined as given in eq 10. In the plot of v versus $[\beta]$ (Figure 10),

$$v = \left(\frac{1 + K_{11}[\beta]}{z}\right)^2 = K_6 + K_6K_{13}[\beta] \qquad (10)$$

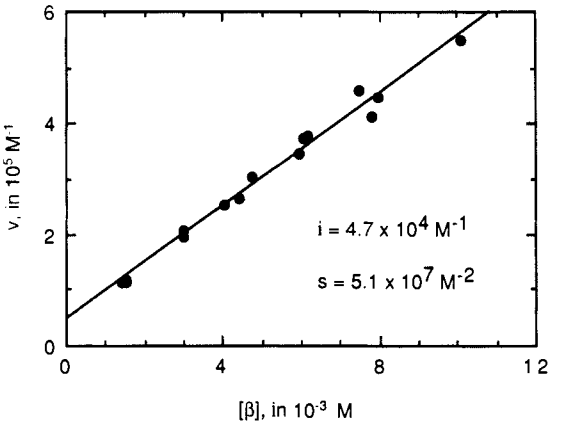

Figure 10. Plot of v versus $[\beta]$. The intercept is equal to K_6 and the slope is equal to the product K_6K_{13}.

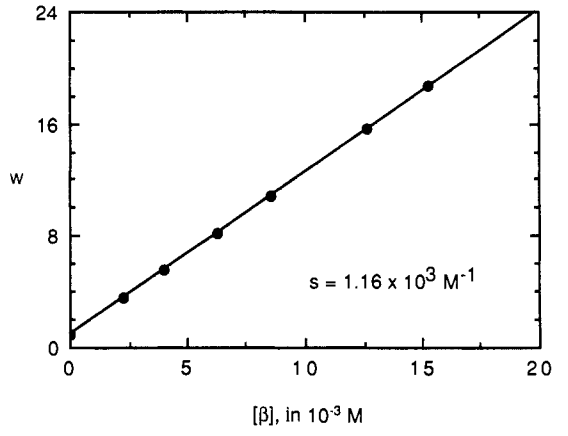

Figure 11. Plot of w versus $[\beta]$. The slope is equal to K_{11}.

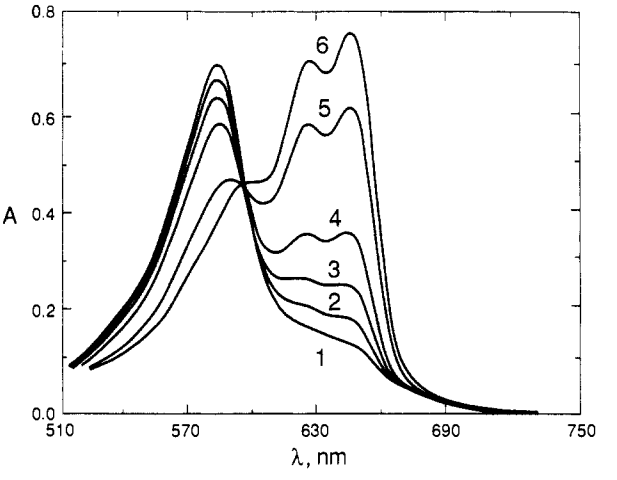

Figure 12. Absorption spectrum of 1.14×10^{-5} M D in the presence of 0.064 M γ-CD in curve 1 and with the addition of 0.0053, 0.012, 0.023, 0.052, and 0.109 M [X] in curves 2, 3, 4, 5, and 6, respectively.

the 5.1×10^7 M^{-2} slope is equal to the product K_6K_{13}, and the 4.7×10^4 M^{-1} intercept is equal to the heretofore elusive K_6; K_{13} must then be equal to 1.09×10^3 M^{-1}. Because $K_6K_{13} = K_{11}K_{12}$ and $K_6K_9 = K_7K_8$, it follows that $K_{12} = 4.9 \times 10^4$ M^{-1} and $K_9 = 1.2 \times 10^6$ M^{-1}.

An additional experiment provides a check on some of these equilibrium constants. To carry out this experiment, whose basis is evident in eq 11, both $[D_0]$ and $[\gamma]$ are kept low and fixed, while

$$w = z(\sqrt{K_6K_9[\gamma] + K_6K_{13}[\beta]}) \approx 1 + K_{11}[\beta] \qquad (11)$$

$[\beta]$ becomes the variable; approximations are the same as applied to eq 9. By plotting w versus $[\beta]$ in Figure 11, we use values for K_6K_9 and K_6K_{13} determined above to redetermine K_{11}. The slope

Scheme III

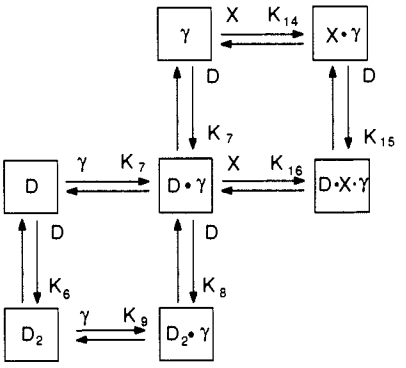

of 1.16×10^3 M^{-1} is within 10% of the value for K_{11} determined from Figure 9.

The alternate method of converting D dimer to D monomer in the presence of γ-CD is to induce coinclusion by adding hexane sulfonate (X) to the solution. Figure 12 shows the effect of increasing concentrations of X on the absorption spectra of solutions containing fixed concentrations of both D and γ-CD. Extensive conversion to monomer D can be effected if enough X is used.

We worked with X earlier as a "filler" molecule that can be coincluded with pyrene butyrate in the γ-CD cavity.[8] Such coinclusion prevents formation of the pyrene ground-state dimer. With D and γ-CD, X appears to function in an analogous manner.

For D together with γ-CD and X, the following equilibrium scheme applies. Three new equilibrium reactions are incorporated in this scheme (Scheme III). Because the concentration of γ-CD was kept relatively low, we did not include the K_{10} equilibrium reaction. Of the three equilibrium reactions occasioned by the presence of X, K_{14} was determined from earlier work[9] to have a value of 20 M^{-1}, so it remained to determine K_{15} and K_{16}.

The parameter z can be related to the concentration of X by the following equation:

$$z = \frac{\sqrt{K_9}(1 + K_7[\gamma] + K_7K_{16}[\gamma][X])}{\sqrt{K_7}(\sqrt{K_8 + K_8K_9[\gamma]})} \qquad (12)$$

The application of this equation to give linear plots permits only one variable, and we selected this to be [X]; this means that [γ], the equilibrium concentration of γ-CD, must be fixed. Since X and γ-CD combine to form 1:1 complexes, any change in the initial concentration of X will, for fixed initial concentrations of γ-CD, also be accompanied by changes in the equilibrium concentrations of γ-CD. To keep these equilibrium concentrations fixed, the initial concentrations of both X and γ-CD must be varied as required by the K_{14} equilibrium reaction.

For our experimental [γ] of 0.0035 M, $K_8 \ll K_8K_9[\gamma]$ and eq 12 can be simplified somewhat. The plot of z versus [X] (Figure 13) has a slope of 0.0205 $M^{-1/2}$ from which we can determine K_{16}

$$z \approx \frac{(1 + K_7[\gamma] + K_7K_{16}[\gamma][X])}{\sqrt{K_7K_8[\gamma]}} \qquad (13)$$

to be 7.4×10^2 M^{-1}. On the basis that $K_7K_{16} = K_{14}K_{15}$, the remaining unknown equilibrium constant K_{15} can be determined to be 4.1×10^3 M^{-1}. Figure 14 summarizes the results of Schemes II and III by listing equilibrium constants and showing ΔG values between the various species.

Fluorescence measurements with solutions of D reveal the monomer form to be essential for detection. When exciting at a common isosbestic point a series of D solutions such as those whose absorption spectra are shown in Figures 7 and 12, the fluorescence levels varied directly with the concentration of D monomer.

(9) Herkstroeter, W. G.; Martic, P. A.; Evans, T. R.; Farid, S. *J. Am. Chem. Soc.* **1986**, *108*, 3275.

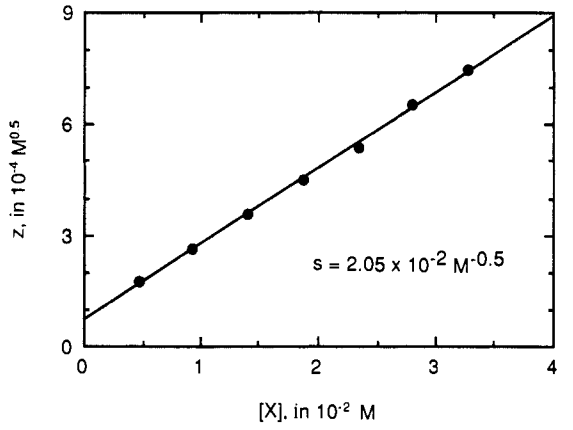

Figure 13. Plot of z versus [X] at a constant equilibrium γ-CD concentration of 0.0035 M.

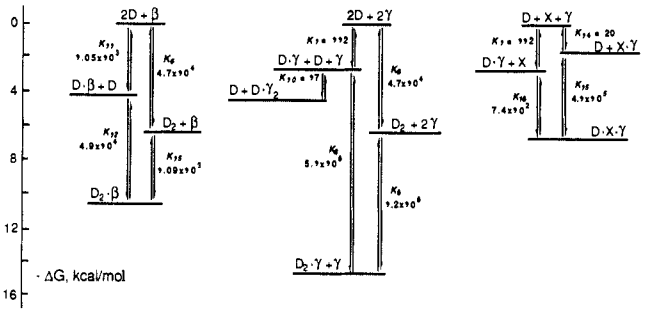

Figure 14. Overall equilibrium Schemes II and III at 25 °C involving D, X, β-CD, and γ-CD and calibrated in terms of ΔG relative to uncomplexed starting reagents.

Discussion

The association of two dye molecules, because of electronic degeneracy, leads to a splitting of the energy levels of the excited states.[10,11] The nature of the molecular association determines the allowed and forbidden transitions. In J-aggregates, the lower energy transition is allowed and the higher energy is forbidden. The opposite is true for H-aggregates, and this is the case we encounter with both A and D. Absorption spectra of the dimers reveal not only the higher energy transitions used to measure solution equilibria but also much weaker transitions to the long wavelength side of the monomer absorption bands.

Whether the dimers that form behave in a manner similar to H- or J-aggregates depends on the relative orientations of the component molecules' transition dipole moments. In H-dimers, these transition dipoles must be parallel to each other and perpendicular to the molecular axes of the individual dimers. Sandwichlike dimers with the component molecules aligned head to head satisfy these requirements.[10,11] Such dimers of A and D constructed from CPK (Corey–Pauling–Koltun) models also meet the spatial requirements predicted by Schemes I, II, and III. Both dimers fill the γ-CD cavity. Although the D dimer is too large for the β-CD cavity, partial insertion in the dimer configuration of only the fused aromatic rings of D can account for our proposed $D_2{\cdot}\beta$ complex. These fused rings almost certainly are the most hydrophobic parts in D and are expected to be attracted by the cavity of β-CD.

Although CPK models predict the existence of all complexes required by our experiments, they say nothing about the relative propensities of each to form. In comparing the equilibrium constants for A and D, two features stand out: corresponding equilibrium constants are larger for D than for A, and equilibrium constants for reactions leading to CD cavities completely filled with dye molecules are larger than for reactions leading to cavities

(10) Herz, A. H. *Photogr. Sci. Eng.* **1974**, *18*, 323.
(11) Herz, A. H. *Theory of the Photographic Process*, 4th ed.; James, T. H., Ed.; Macmillan: New York, 1977; pp 218–222.

only partially filled with dye molecules. This observation is in agreement with other reports of dye dimer formation within γ-CD cavities.[12-16]

The larger equilibrium constants for D than for A can be attributed at least in part to the more hydrophobic nature of the former, as demonstrated by comparing K_6 and K_1. Because D is more hydrophobic, it has a greater propensity not only to dimerize but also to seek out the sheltered environments of CD cavities. The hydrophobic interactions between guest and host, however, are not maximized unless all water molecules are displaced and the cavities are completely filled with dye molecules.

The present study clearly demonstrates that proper size matching between the guest and the host's cavity leads to substantially larger equilibrium constants.[17] As an example, K_{11} for the inclusion of one D molecule in β-CD (1.05×10^3 M^{-1}) is higher than that for inclusion in γ-CD ($K_7 = 1.12 \times 10^2$ M^{-1}), where, because of the looser fit, more water molecules are retained. The inclusion of D in γ-CD is, however, considerably enhanced when the cavity is partially filled with a molecule of X. The equilibrium constant K_{15} of 4.1×10^3 M^{-1} for inclusion of D in X·γ is even larger than for inclusion in β-CD. With D in dimer form, the cavity of γ-CD provides for the better fit as shown by the equilibrium constant K_9 (1.2×10^6 M^{-1}) being over three orders of magnitude larger than K_{13} (1.09×10^3 M^{-1}) for inclusion of D_2 in the cavity of β-CD. The cavity of γ-CD can enclose D_2 snugly with good protection from the aqueous environment, whereas the cavity of β-CD is undersized for D_2 and partial penetration does not displace all of the water molecules.

Another example is provided by comparing the inclusion of X by γ-CD and D·γ. Because the cavity of the former is too spacious for a single molecule of X, the equilibrium constant for the formation of X·γ is relatively weak ($K_{14} = 20$ M^{-1}). Inclusion of X in the much smaller space left in the D·γ complex results in a large increase in the equilibrium constant ($K_{16} = 7.4 \times 10^2$ M^{-1}).

Additional information is provided through comparison of the thermodynamic parameters ΔH and ΔS. For such comparisons, however, our data are limited to the reactions of K_1 through K_4.

Negative enthalpy changes should result from hydrophobic interactions of dye molecules with CD cavity walls.[18,19] Displacing water molecules by dye molecules inside CD cavities should have a positive entropy change, whereas negative entropy changes are expected when complexation places restrictions to rotation on the host CD.[18,19]. The special alignment required to form tightly packed inclusion complexes may also contribute to negative entropy changes.

For K_1, the negative ΔH is undoubtedly caused by the hydrophobic attractions of two A molecules for each other, whereas the negative ΔS can be attributed to restricted rotation of the complex once formed. The reaction corresponding to K_2 involves partial displacement of water molecules from the interior of γ-CD by a single molecule of A. One molecule of A inside γ-CD leaves considerable space that will, of necessity, be occupied by water molecules. Hydrophobic attractions must be minimal, as reflected by an immeasurably small ΔH. The positive ΔS measured for this reaction must be caused by displacement by A of some of the water molecules from the interior of γ-CD. For A·γ, this positive ΔS is more than enough to override the expected negative contribution caused by special alignment in formation and restricted rotation relative to free γ-CD. A number of examples of CD complexation equilibria with positive ΔS's have been reported.[1,4,17-26]

For K_3 and K_4, the negative contributions to both ΔH and ΔS become dominant. Judging from the relative magnitudes of these thermodynamic parameters, the hydrophobic attractions involved with K_3 must be larger than with K_4, and they can be rationalized in terms of both dye–dye and dye–cavity hydrophobic interactions in the K_3 reaction, but only in terms of the latter in the K_4 reaction. As far as the entropy change is concerned, both reactions lead to A_2·γ, so the restriction to rotation of the product should be the same for both reactions. However, the different ΔS values can be accounted for in terms of water displacement; the reaction of K_3 displaces less water than the reaction of K_4.

Both A and D are laser dyes and, as such, are known to fluoresce with high quantum yields.[27] For each dye, however, we have seen that fluorescence quantum yields in monomer–dimer mixtures are directly proportional to the fraction of monomer present. That the dimers do not fluoresce is a direct consequence of their H-dimer configurations and the forbidden nature of transitions between the lowest excited singlet states and the ground states. With A in aqueous solution and with no CDs present, fluorescence losses due to dimerization would be significant for concentrations of 1×10^{-4} M and higher, but, for D, such losses would occur even for concentrations below 1×10^{-6} M. Because of lowered fluorescence yields in water, laser dyes are usually used in organic solvents such as alcohols where measurable dimerization does not occur. Dye inclusion or coinclusion in the proper CD, however, can lead to monomerization and, hence, efficient fluorescence even in concentrated aqueous solutions.[28]

Experimental Section

Amphiphile X was Kodak HPLC grade and was recrystallized from ethanol. The remaining reagents, Kodak laser grade A and D along with β- and γ-CD from Sigma Chemical Co., were used as received. Deionized water was passed through a Milli-Q system from Millipore Corp.; this water with added 2×10^{-5} M NaOH was used as solvent in all experiments.

Absorption spectra were measured on a Hitachi Perkin-Elmer Model 320 spectrophotometer equipped with temperature-controlled cell holders.

Registry No. A, 24796-94-9; D, 61318-65-8; γ-CD, 17465-86-0; β-CD, 7585-39-9.

(12) Clarke, R. J.; Coates, J. H.; Lincoln, S. F. *Carbohydr. Res.* **1984**, *127*, 181.
(13) Schiller, R. L.; Coates, J. H.; Lincoln, S. F. *J. Chem. Soc., Faraday Trans. I* **1984**, *80*, 1257.
(14) Clarke, R. J.; Coates, J. H.; Lincoln, S. F. *J. Chem. Soc., Faraday Trans. I* **1984**, *80*, 3119.
(15) Schiller, R. L.; Lincoln, S. F.; Coates, J. H. *J. Chem. Soc., Faraday Trans. I* **1986**, *82*, 2123.
(16) Schiller, R. L.; Lincoln, S. F.; Coates, J. H. *J. Inclusion Phenom.* **1987**, *5*, 59.
(17) Cf.: Cromwell, W. C.; Byström, K.; Eftink, M. R. *J. Phys. Chem.* **1985**, *89*, 326.
(18) Bergeron, R. J.; Pillor, D. M.; Gibeily, G.; Roberts, W. P. *Biorg. Chem.* **1978**, *7*, 263.
(19) Bergeron, R. J. In *Inclusion Compounds*; Atwood, J. L., Davies, J. E. D., MacNichol, D. D., Eds.; Academic: New York, 1984; pp 423–429.
(20) Tabushi, I.; Klyosucke, Y.; Sugimoto, T.; Yamamura, K. *J. Am. Chem. Soc.* **1978**, *100*, 916.
(21) Matsui, Y.; Mochida, K. *Bull. Chem. Soc. Jpn.* **1979**, *52*, 2808.
(22) Gerasimowicz, W. V.; Wojcik, J. F. *Biorg. Chem.* **1982**, *11*, 420.
(23) Hersey, A.; Robinson, B. H. *J. Chem. Soc., Faraday Trans. I* **1984**, *80*, 2039.
(24) Kasatani, K.; Kawasak, M.; Sato, H. *J. Phys. Chem.* **1984**, *88*, 5451.
(25) Bright, F. V.; Keimig, T. L.; McGown, L. B. *Anal. Chim. Acta* **1985**, *175*, 189.
(26) Briggner, L. E.; Ni, X. R.; Tempesti, F.; Wadsoe, I. *Thermochim. Acta* **1986**, *109*, 139.
(27) Sens, R.; Drexhage, K. H. *J. Lumin.* **1981**, *24–25*, 709.
(28) Cf.: Degani, Y.; Willner, I.; Haas, Y. *Chem. Phys. Lett.* **1984**, *104*, 496.